Structural complexity and metal coordination flexibility in two acetophosphonates

Aurelio Cabeza, Miguel A. G. Aranda and Sebastian Bruque*

Departamento de Química Inorgánica, Cristalografía y Mineralogía, Universidad de Málaga, 29071 Málaga, Spain. E-mail: bruque@uma.es

Two divalent metal acetophosphonates, $Pb_6(O_3PCH_2CO_2)_4$ and $Mn_3(O_3PCH_2CO_2)_2$, have been synthesised hydrothermally. They crystallise in the triclinic system, space group $P\bar{1}$, $a = 11.0064(1)$, $b = 12.3604(1)$, $c = 8.9783(1)$ Å, $\alpha = 98.632(1)$, $\beta = 90.474(1)$, $\gamma = 75.629(1)°$, $Z = 2$, for M = Pb, and $a = 10.0146(5)$, $b = 6.3942(4)$, $c = 8.4796(6)$ Å, $\alpha = 101.452(4)$, $\beta = 106.254(2)$, $\gamma = 96.431(4)°$, $Z = 2$, for M = Mn. The structures were solved *ab initio* using direct methods from synchrotron powder diffraction data ($\lambda \approx 0.4$ Å) for M = Pb and from laboratory X-ray data for M = Mn. The crystal structure of the Pb compound is very complex with 38 non-hydrogen atoms in general positions (114 refined positional parameters), it had been refined by Rietveld method using soft constraints, and converged to $R_{WP} = 6.8\%$ and $R_F = 1.6\%$. The structure for M = Mn has a moderate complexity with 19 non-hydrogen atoms (57 refined positional parameters) which was also refined with soft constraints to $R_{WP} = 8.3\%$, $R_F = 3.9\%$. Both compounds show a framework built of alternate metal oxide inorganic layers, pillared by the organic groups. The metal environments in these materials are very distorted. Manganese atoms present three different distorted oxygen environments: four-, five- and six-coordinate. Thermal and IR data are also reported and discussed.

Introduction

The interest in the chemistry of phosphonates has drastically increased in the last twenty years.[1] Initially, these compounds (with phosphonic acid H_2O_3PR, R = alkyl or aryl group) were mainly layered with structures very related to that of the parent zirconium hydrogen phosphate a-$Zr(HPO_4)_2 \cdot H_2O$.[2] The ability to design structures with specific properties that these materials show, as well as their unusual compositional and structural diversity varying from one-dimensional arrangements[3,4] to three-dimensional microporous frameworks,[5–7] *via* the most common layered frameworks,[8–10] have stimulated extensive exploration of their chemistry. In fact, the importance of such systems in several research areas such as electrochemistry,[11,12] microelectronic,[13] photochemical mechanisms[14] and catalysis[15,16] has been widely recognised.

Metal phosphonates with 3D frameworks can be synthesised as nanotubular phosphonates or alternatively as pillared layered structures (PLS) by using, for example, diphosphonic acids $H_2O_3P–R–PO_3H_2$ as pillaring agent.[17] Hence, it is possible to design the interlayer spacing (and chemistry) through the shape, size and nature of the organic spacer R. Several other ways to obtain PLS materials have also been adopted, *e.g.* use of carboxyphosphonates,[18] or through the reaction of free hydrogen carboxyphosphonate groups with intercalated alkyl diamines $H_2N–R–NH_2$ at high temperature which yields covalent amide links.[19]

The synthesis and structures of several 2-carboxyethylphosphonates of divalent and trivalent metals have been reported. For example, Fe phosphonates,[20a] $Fe^{III}(HO_3PR)_3(H_2O_3PR)$, $Fe^{II}(HO_3PR)_2$, $Fe^{III}(HO_3PR)(O_3PR) \cdot H_2O$ and $Fe^{III}O(HO_3PR) \cdot H_2O$, with R = $C_2H_4CO_2H$; Bi phosphonates,[18c] $Bi(O_3PC_2H_4CO_2) \cdot H_2O$ and $Bi(HO_3PC_2H_4CO_2H)(O_3PC_2H_4CO_2H)$; and even bimetallic phosphonates,[20b] $MnZn_2(O_3PC_2H_4CO_2)_2$, as well as $Mn(O_3PC_2H_4CO_2H) \cdot H_2O$ and $Mn_3(O_3PC_2H_4CO_2)_2$. The structures of most of these compounds exhibit inorganic layers formed by the metal cations and the PO_3 and CO_2 moieties, pillared by the organic groups to yield 3D frameworks. The metal environments are very versatile in these materials as has been shown for $Zn_3(O_3PC_2H_4CO_2)_2$,[18b] where there are two tetrahedral and one octahedral sites for the zinc atoms. As yet, the structure of $Mn_3(O_3PC_2H_4CO_2)_2$ has not been solved, although it seems to be isostructural to the Zn analog.[20b] The synthesis and structure of $Co_3(O_3PC_2H_4CO_2)_2 \cdot 6H_2O$ has very recently been reported exhibiting a 3D 'open' framework.[21]

In this paper, we report the synthesis, characterisation and crystal structure of two acetophosphonates, $Pb_6(O_3PCH_2CO_2)_4$ and $Mn_3(O_3PCH_2CO_2)_2$.

Experimental

Synthesis of $Mn_3(O_3PCH_2CO_2)_2$

Chemicals of reagent quality were obtained from Aldrich and used without purification. Manganese(II) acetophosphonate was synthesised by adding 1.43 mmol manganese(II) acetate tetrahydrate dissolved in 10 ml distilled water to an aqueous solution (10 ml) containing 7.14 mmol acetophosphonic acid; the resulting Mn:P molar ratio was 1:5 and the solution has a pH of 1.4. No precipitate is formed even on hydrothermally heating at 150 °C for one week thus the pH of the solution was increased by adding 30% aqueous NaOH dropwise up to pH 4.3. At this point, a precipitate started to develop.

This suspension was heated again in a Teflon-lined autoclave at 150 °C for 5 days. A single powdered phase was filtered, washed with water and with acetone, and dried under vacuum.

Synthesis of $Pb_6(O_3PCH_2CO_2)_4$

Lead acetophosphonate was also prepared hydrothermally. 4.08 mmol acetophosphonic acid were dissolved in 10 ml distilled water. A second solution containing 0.816 mmol of lead acetate trihydrate dissolved in 15 ml of water was added slowly and with constant stirring. The resulting Pb:P molar ratio of 1:5 and a pH of 1.4. Under these conditions, no precipitate formed; thus as described above, the pH was increased up to 1.8, leading to the formation of a white precipitate. This mixture was heated in a Teflon-lined autoclave at 150 °C for 6 days. A single powdered phase was isolated by filtration, washed with water and acetone, and finally dried under vacuum.

Elemental analysis. Carbon and hydrogen contents were determined by elemental chemical analysis on a Perkin-Elmer 240 analyser. Analytical data for $Mn_3(O_3PCH_2CO_2)_2$: C, 10.54; H, 0.95. Calc.: C, 10.94; H, 0.91%. Analytical data for $Pb_6(O_3PCH_2CO_2)_4$: C, 5.20; H, 0.45. Calc.: C, 5.35; H, 0.45%.

Thermal analysis. TGA and DTA data were collected on a Rigaku Thermoflex apparatus at a heating rate of 10 K min^{-1} in air with calcined Al_2O_3 as an internal reference standard.

IR study. IR spectra were recorded on Perkin Elmer 883 spectrometer in the spectral range 4000–400 cm^{-1}, using dry KBr pellets containing 2% of sample.

X-Ray powder diffraction. The powder diffraction pattern for $Mn_3(O_3PCH_2CO_2)_2$ were collected on a Siemens D-5000, automated diffractometer using graphite-monochromated Cu-Kα radiation. The sample was diluted and blended with spherical particles of Cab-O-Sil M-5 (Fluka), to reduce preferred orientations.[22] The angular range scanned was 7–80° (2θ), with a step size of 0.02° and counting time of 20 s per step.

For $Pb_6(O_3PCH_2CO_2)_4$, high resolution synchrotron powder data were collected on the diffractometer of the BM16 line of ESRF (Grenoble, France). The sample was loaded in a borosilicate glass capillary (diameter = 0.5 mm) and rotated during data collection. The pattern was collected with $\lambda = 0.399\,89(2)$ Å, in the angular range 1–30° in 2θ, for an overall count time of 10 h. Raw data were normalised and reduced to a constant step size of 0.003° with local software. Further experimental details about data collection and analysis of this type of data have been already reported.[23]

Results and discussion

Thermal study

TGA–TDA curves for $Mn_3(O_3PCH_2CO_2)_2$ and $Pb_6(O_3PCH_2CO_2)_4$ are shown in Fig. 1. Only one exothermic effect, with an abrupt change in the DTA curve, was observed for both compounds. For $Mn_3(O_3PCH_2CO_2)_2$ the exotherm takes place at higher temperature (570 °C) than for $Pb_6(O_3PCH_2CO_2)_4$ (418 °C). This effect is due to the combustion of the acetocarboxylic groups and it has an associated mass loss of 18.5 and 11.0%, for M = Mn and Pb, respectively. These values are in good agreement with theoretical values (19.14 and 9.38%, respectively) calculated for the following

thermal decomposition reactions:

$$Mn_3(O_3PCH_2CO_2)_2 + 4O_2 \rightarrow Mn_3(PO_4)_2 + 4CO_2 + 2H_2O$$
$$Pb_6(O_3PCH_2CO_2)_4 + 8O_2 \rightarrow 2Pb_3(PO_4)_2 + 8CO_2 + 4H_2O$$
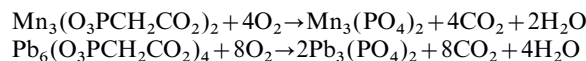
The thermal decomposition products were identified through the powder patterns collected for the samples heated at 1000 °C. This high temperature was used to increase crystallinity which helps in the identification procedure. The patterns matched with those present in the PDF database: no. 31-0827 for $Mn_3(PO_4)_2$ and 24-0585 for $Pb_3(PO_4)_2$.

IR spectroscopy study

The IR spectra of both compounds are shown in Fig. 2. There are no bands in the O–H stretching region (3500–3000 cm^{-1}), which is consistent with the absence of water molecules or hydrogen phosphonate/carboxylate groups in the structures. As it can be observed in Fig. 2, no band is seen at ca. 1715 cm^{-1} corresponding to ν(C=O) for the free acid (–COOH). However, there are two pairs of strong bands centred at 1610, 1550 and 1425, 1380 cm^{-1}, for $Mn_3(O_3PCH_2CO_2)_2$, and at 1550, 1505 cm^{-1} and 1420, 1370 cm^{-1}, for $Pb_6(O_3PCH_2CO_2)_4$, which are assigned to the antisymmetrical and symmetrical stretching vibrations of C–O groups when present as COO$^-$ moieties.[24] There are two set of bands probably due to crystallographically different carboxylic groups coordinated to the metal atoms, as has been confirmed by XRD. Other bands characteristic of the phosphonate groups are also present in the IR spectra.

Structure determination

The X-ray laboratory powder pattern for $Mn_3(O_3PCH_2CO_2)_2$ was auto-indexed using the TREOR90 program[25] giving a triclinic unit cell with $a = 10.001$, $b = 6.379$, $c = 8.478$ Å, $\alpha = 101.39$, $\beta = 106.32$, $\gamma = 96.38°$, $V = 500.8$ Å^3, $Z = 2$, V_{at} (non-H atoms) = 13.2 Å^3 atom^{-1}, $M_{20} = 33$[26] and $F_{20} = 55$ (0.0085, 43).[27] The X-ray synchrotron powder pattern for $Pb_6(O_3PCH_2CO_2)_4$ was auto-indexed by the TREOR90[25] program in a triclinic unit cell with dimensions: $a = 11.002$, $b = 12.365$, $c = 8.984$ Å, $\alpha = 98.68$, $\beta = 90.49$, $\gamma = 75.64°$, $V = 1170.0$ Å^3, $Z = 2$, $V_{at} = 15.38$ Å^3 atom^{-1}, $M_{20} = 48$[26] and $F_{20} = 161$ (0.0048, 26).[27] Both crystal structures were solved by ab initio procedures. The pattern decomposition option of the GSAS package[28] was used to extract corrected structure factors, using the Le Bail method,[29] from a limited region of the pattern, $14 < 2\theta < 62°$ for Mn compound (650 reflections) and $1.5 < 2\theta < 20.5°$, for Pb compound (1500 reflections). The
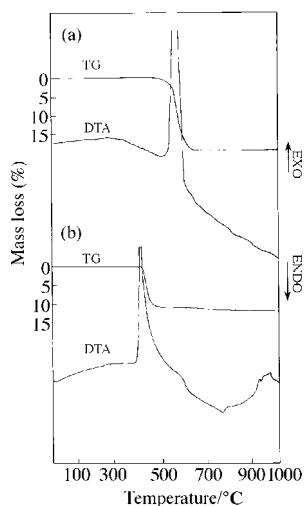
Fig. 1 TGA-DTA curves for (a) $Mn_3(O_3PCH_2CO_2)_2$ and (b) $Pb_6(O_3PCH_2CO_2)_4$.
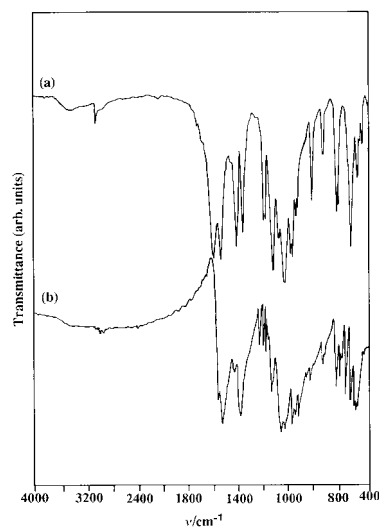
Fig. 2 IR spectra for (a) $Mn_3(O_3PCH_2CO_2)_2$ and (b) $Pb_6(O_3PCH_2CO_2)_4$.
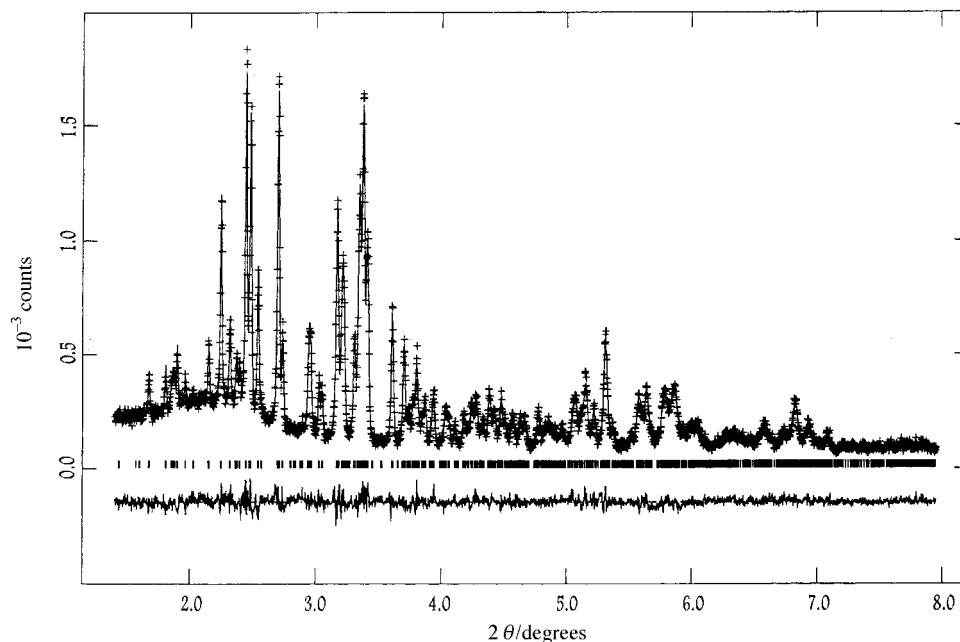
Fig. 3 Observed, calculated and difference X-ray powder diffraction profiles for $Mn_3(O_3PCH_2CO_2)_2$. The tick marks are calculated 2θ angles for Bragg peaks.

patterns were fitted without any structural model by refining the overall parameters: background, zero-point error, unit cell and peak shape values. A pseudo-Voigt peak shape function[30] corrected for asymmetry[31] was used. SIRPOW92[32] gave the positions of three manganese atoms and two phosphorus atoms by direct methods. SHELXS86[33] gave the positions of the six lead atoms by both Patterson map and direct methods. For both compounds, the found atoms were included in the Rietveld refinements using the overall parameters obtained in the last cycle of the *ab initio* refinements. R_{wP} dropped to 23.6% for M = Pb and to 32.0% for M = Mn by refining only the scale factors. Successive difference Fourier maps and soft constrained refinements led to the atomic positions of the remaining atoms. It is worthy to underline that due to the complexity of these structures, the atomic positions were refined using the following soft constraints, P–O [1.53(1) Å],

P–C [1.80(1) Å], O···O [2.55(1) Å], O···O [2.73(1) Å], C–C_{carb} [1.50(1) Å], C_{carb}–O_{carb} [1.23(1) Å], C···O_{carb} [2.36(1) Å] and O_{carb}···O_{carb} [2.15(1) Å], to retain a reasonable geometry for the tetrahedral O_3PC and carboxylic groups. The final weights for the soft constraints were −10. The powder pattern collected in $\theta/2\theta$ geometry for M = Mn showed a strong preferred orientation along the [010] and [100] directions, which were corrected using the March–Dollase[34] function with coefficients of 1.147(7) for [010] and 0.666(6) for [100]. The synchrotron powder pattern collected on a capillary for M = Pb did not show preferred orientation. The final refinement for $Mn_3(O_3PCH_2CO_2)_2$ converged to R_{wP} = 8.29%, R_P = 6.43% and R_F = 3.91%; and for $Pb_6(O_3PCH_2CO_2)_4$ to R_{wP} = 6.76%, R_P = 5.22% and R_F = 1.64%; R factors are defined by Rietveld,[35] and Larson and Von Dreele.[28] The Rietveld plots for Mn and Pb compounds are shown in Fig. 3 and 4,
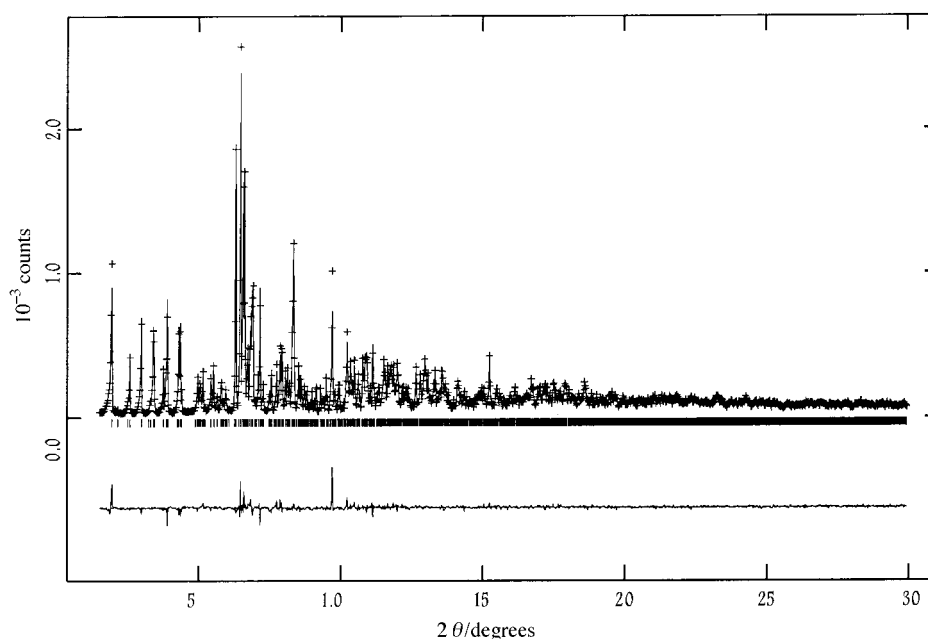
Fig. 4 Observed, calculated and difference synchrotron X-ray ($\lambda \approx 0.4$ Å) powder diffraction profiles for $Pb_6(O_3PCH_2CO_2)_4$ between 1.5 and 30° (2θ). The tick marks are calculated 2θ angles for Bragg peaks.

Table 1 Positional parameters for $Mn_3(O_3PCH_2CO_2)_2$ in space group $P\bar{1}$

Atom	x	y	z	$U_{iso}/\text{Å}^2$
Mn(1)	0.4490(4)	0.0986(9)	0.8271(6)	0.017(2)
Mn(2)	0.1209(5)	0.8001(10)	0.5498(8)	0.032(2)
Mn(3)	0.3827(5)	0.6098(11)	0.3819(6)	0.022(2)
P(1)	0.6856(7)	0.9316(14)	0.6480(8)	0.044(4)
P(2)	0.3651(7)	0.5789(13)	0.7877(10)	0.027(3)
O(1)	0.6212(11)	1.1134(19)	0.7346(13)	0.014(2)
O(2)	0.5839(11)	0.7120(17)	0.5985(15)	0.014
O(3)	0.7177(13)	0.9879(23)	0.4927(12)	0.014
O(4)	0.2851(11)	0.6070(12)	0.6098(12)	0.014
O(5)	0.4682(10)	0.4203(18)	0.7756(17)	0.014
O(6)	0.4398(10)	0.8000(15)	0.9083(15)	0.014
O(7)	0.9902(12)	0.6850(23)	0.6842(22)	0.014
O(8)	0.8228(15)	0.5306(21)	0.7581(22)	0.014
O(9)	0.2318(15)	0.0852(20)	0.8128(18)	0.014
O(10)	0.0533(12)	0.1953(24)	0.6658(18)	0.014
C(1)	0.8496(10)	0.9099(20)	0.7968(15)	0.008(5)
C(2)	0.8891(20)	0.6936(19)	0.7397(33)	0.008
C(3)	0.2329(11)	0.4619(18)	0.8705(15)	0.008
C(4)	0.1619(15)	0.2302(19)	0.7876(22)	0.008
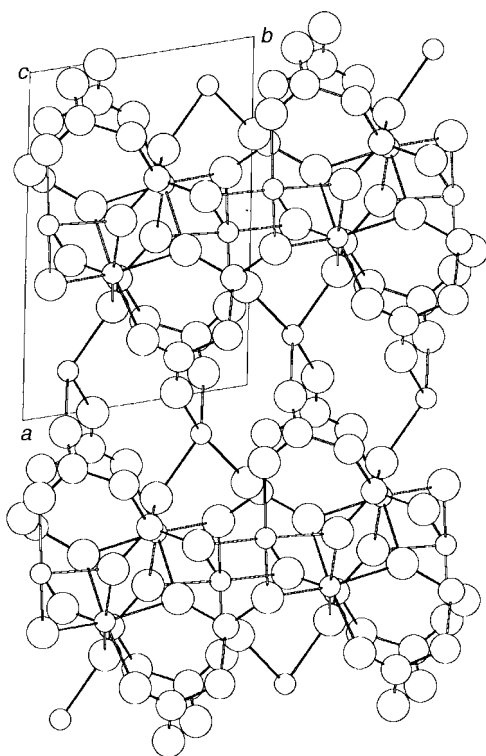
respectively. Atomic parameters are presented in Table 1 and bond lengths in Table 2 for M = Mn, and in Table 3 and 4 for M = Pb, respectively.

Attempts to solve the structure of $Pb_6(O_3PCH_2CO_2)_4$ from laboratory X-ray powder data were unsuccessful. Thus, a synchrotron pattern was collected owing to the high quality of diffraction data, utilising the very high angular resolution and the absence of preferred orientation. Under these conditions, with better structure factors, such a complex structure (38 non-hydrogen atoms in the asymmetric part of the unit cell including six crystallographically independent lead atoms) could be successfully solved from powder diffraction data.

Structure description

The crystal structure of $Mn_3(O_3PCH_2CO_2)_2$ contains 19 non-hydrogen atoms in the asymmetric unit of the unit cell,

Table 3 Positional parameters for $Pb_6(O_3PCH_2CO_2)_4$ in space group $P\bar{1}$

Atom	x	y	z	$U_{iso}/\text{Å}^2$
Pb(1)	0.33231(30)	0.29920(27)	0.91369(32)	0.0111(9)
Pb(2)	−0.00392(28)	0.49459(25)	0.23407(31)	0.0081(9)
Pb(3)	0.17993(28)	0.69240(27)	0.50670(31)	0.0055(8)
Pb(4)	0.50768(29)	0.50721(25)	0.73390(30)	0.0059(9)
Pb(5)	0.39799(28)	0.87470(26)	0.77513(33)	0.0113(9)
Pb(6)	0.11856(29)	0.11283(27)	0.08619(31)	0.0204(10)
P(1)	0.2555(14)	0.4298(12)	0.5390(15)	0.006(2)
P(2)	0.7553(14)	0.4389(12)	−0.0656(14)	0.006
P(3)	0.5803(14)	0.0665(13)	0.8220(15)	0.006
P(4)	0.0900(13)	0.0029(11)	0.7295(14)	0.006
O(1)	0.2434(27)	0.4115(21)	0.7048(15)	0.006
O(2)	0.3625(20)	0.4870(22)	0.5195(29)	0.006
O(3)	0.1299(18)	0.5001(20)	0.4887(30)	0.006
O(4)	0.3979(24)	0.3001(33)	0.1981(29)	0.006
O(5)	0.2017(26)	0.3019(34)	0.1846(29)	0.006
O(6)	0.8684(21)	0.4867(23)	−0.0129(31)	0.006
O(7)	0.6337(20)	0.5102(20)	1.0190(28)	0.006
O(8)	0.7415(26)	0.4337(20)	0.7620(16)	0.006
O(9)	0.8882(26)	0.3109(33)	0.2086(30)	0.006
O(10)	0.6940(25)	0.3074(34)	0.2191(29)	0.006
O(11)	0.5839(28)	0.1399(21)	0.9763(20)	0.006
O(12)	0.3439(24)	0.0569(14)	0.1757(28)	0.006
O(13)	0.5568(16)	0.9301(26)	0.2210(30)	0.006
O(14)	0.5240(33)	0.3048(22)	0.7667(31)	0.006
O(15)	0.6004(34)	0.2736(22)	0.5403(27)	0.006
O(16)	0.0417(15)	0.9513(23)	0.1959(27)	0.006
O(17)	0.8087(20)	0.0264(23)	0.1525(25)	0.006
O(18)	0.9049(28)	0.1020(15)	0.3916(23)	0.006
O(19)	0.8962(33)	0.7474(24)	0.1525(25)	0.006
O(20)	−0.0199(33)	0.6963(21)	0.3555(33)	0.006
C(1)	0.2925(30)	0.2924(14)	0.4223(20)	0.006
C(2)	0.2963(25)	0.305(4)	0.2586(24)	0.006
C(3)	0.7845(29)	0.2963(13)	0.9779(22)	0.006
C(4)	0.7901(27)	0.302(5)	0.1457(23)	0.006
C(5)	0.6523(26)	0.1229(19)	0.6810(30)	0.006
C(6)	0.595(4)	0.2444(21)	0.6650(28)	0.006
C(7)	0.1257(30)	0.1115(15)	0.6344(26)	0.006
C(8)	0.082(5)	0.2308(21)	0.7132(30)	0.006

Fig. 5 [001] View of the crystal structure of $Mn_3(O_3PCH_2CO_2)_2$.

Table 2 Bond lengths (Å) for $Mn_3(O_3PCH_2CO_2)_2$. Long Mn–O interactions are given in italics

Mn(1)−O(1)	2.085(12)	Mn(1)−O(6)	2.156(12)	Mn(1)−O(9)	2.135(15)
Mn(1)−O(5)	2.185(11)	Mn(1)−O(6)	2.134(12)	*Mn(1)−O(3)*	*2.667(10)*
Mn(2)−O(3)	2.147(11)	Mn(2)−O(7)	2.123(14)	*Mn(2)−O(9)*	*2.465(14)*
Mn(2)−O(4)	2.173(13)	Mn(2)−O(10)	2.153(13)	*Mn(2)−O(10)*	*2.753(14)*
Mn(3)−O(1)	2.190(13)	Mn(3)−O(4)	2.399(11)	*Mn(3)−O(3)*	*2.975(15)*
Mn(3)−O(2)	2.240(11)	Mn(3)−O(5)	2.265(11)		
Mn(3)−O(2)	2.152(11)	Mn(3)−O(8)	2.060(15)		
P(1)−O(1)	1.550(5)	P(2)−O(4)	1.554(5)		
P(1)−O(2)	1.547(5)	P(2)−O(5)	1.535(5)		
P(1)−O(3)	1.538(5)	P(2)−O(6)	1.538(5)	C(1)−C(2)	1.506(6)
P(1)−C(1)	1.808(5)	P(2)−C(3)	1.820(5)	C(2)−O(7)	1.232(5)
				C(2)−O(8)	1.232(5)
C(3)−C(4)	1.505(6)	C(4)−O(9)	1.240(6)	C(4)−O(10)	1.235(6)

Table 4 Bond lengths (Å) for $Pb_6(O_3PCH_2CO_2)_4$. Long Pb–O interactions are given in italics and the average Pb–O distance for each polyhedron (coordination number as subscript) are also given

Pb(1)—O(1)	2.55(2)	Pb(1)—O(7)	2.46(3)	Pb(1)—O(19)	2.76(4)
Pb(1)—O(4)	2.65(3)	Pb(1)—O(11)	3.08(3)	*Pb(1)—O(8)*	*3.98(2)*
Pb(1)—O(5)	2.83(3)	Pb(1)—O(13)	2.88(3)	*Pb(1)—O(20)*	*4.18(3)*
Pb(1)—O(6)	3.02(3)	Pb(1)—O(14)	2.52(3)	$<Pb(1)-O_9>$	2.75
Pb(2)—O(1)	2.63(3)	Pb(2)—O(6)	2.62(2)	*Pb(2)—O(8)*	*3.22(3)*
Pb(2)—O(3)	2.71(2)	Pb(2)—O(6)	2.57(3)	*Pb(2)—O(9)*	*3.24(3)*
Pb(2)—O(3)	2.84(3)	Pb(2)—O(20)	2.53(3)	*Pb(2)—O(19)*	*4.19(4)*
Pb(2)—O(5)	2.83(4)	Pb(2)—O(9)	2.79(3)	$<Pb(2)-O_8>$	2.69
Pb(3)—O(2)	2.84(3)	Pb(3)—O(10)	2.82(3)	*Pb(3)—O(1)*	*4.04(2)*
Pb(3)—O(3)	2.55(3)	Pb(3)—O(15)	2.60(4)		
Pb(3)—O(8)	2.69(2)	Pb(3)—O(18)	2.51(2)		
Pb(3)—O(9)	2.68(3)	Pb(3)—O(20)	2.57(3)	$<Pb(3)-O_8>$	2.66
Pb(4)—O(2)	2.51(3)	Pb(4)—O(7)	2.79(2)	Pb(4)—O(15)	3.08(3)
Pb(4)—O(2)	2.72(2)	Pb(4)—O(8)	2.53(3)	*Pb(4)—O(1)*	*3.39(3)*
Pb(4)—O(4)	2.81(4)	Pb(4)—O(10)	2.75(4)	*Pb(4)—O(15)*	*3.89(2)*
Pb(4)—O(7)	2.90(3)	Pb(4)—O(14)	2.53(3)	$<Pb(4)-O_9>$	2.73
Pb(5)—O(4)	2.74(3)	Pb(5)—O(17)	2.35(2)	*Pb(5)—O(12)*	*3.91(1)*
Pb(5)—O(10)	2.69(4)	*Pb(5)—O(15)*	*3.13(3)*		
Pb(5)—O(11)	2.27(2)	*Pb(5)—O(12)*	*3.17(3)*		
Pb(5)—O(13)	2.58(3)	*Pb(5)—O(18)*	*3.61(3)*	$<Pb(5)-O_5>$	2.53
Pb(6)—O(5)	2.74(4)	Pb(6)—O(19)	2.93(3)	*Pb(6)—O(18)*	*3.67(3)*
Pb(6)—O(12)	2.56(3)	*Pb(6)—O(9)*	*3.13(4)*	*Pb(6)—O(11)*	*3.91(3)*
Pb(6)—O(16)	2.67(3)	*Pb(6)—O(16)*	*3.19(3)*		
Pb(6)—O(17)	2.54(3)	*Pb(6)—O(17)*	*3.67(3)*	$<Pb(6)-O_5>$	2.69
P(1)—O(1)	1.551(7)	P(2)—O(6)	1.547(7)	P(3)—O(11)	1.543(7)
P(1)—O(2)	1.540(7)	P(2)—O(7)	1.541(7)	P(3)—O(12)	1.550(7)
P(1)—O(3)	1.543(7)	P(2)—O(8)	1.548(7)	P(3)—O(13)	1.546(7)
P(1)—C(1)	1.810(8)	P(2)—C(3)	1.813(8)	P(3)—C(5)	1.809(7)
P(4)—O(16)	1.538(7)	C(1)—C(2)	1.502(8)	C(3)—C(4)	1.499(8)
P(4)—O(17)	1.546(7)	C(2)—O(4)	1.233(8)	C(4)—O(9)	1.236(8)
P(4)—O(18)	1.553(7)	C(2)—O(5)	1.235(8)	C(4)—O(10)	1.233(8)
P(4)—C(7)	1.815(8)				
C(5)—C(6)	1.506(8)	C(6)—O(14)	1.231(8)	C(8)—O(19)	1.230(7)
C(6)—O(15)	1.233(8)	C(7)—C(8)	1.498(8)	C(8)—O(20)	1.231(7)
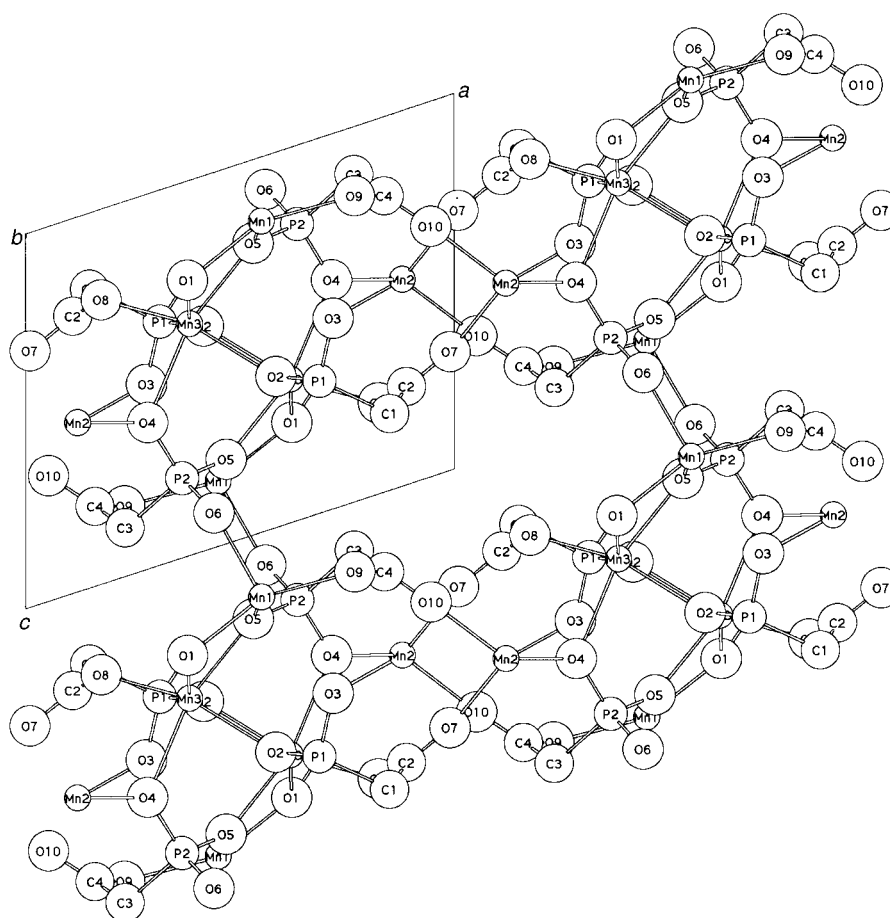
Fig. 6 [010] View of the crystal structure of $Mn_3(O_3PCH_2CO_2)_2$ with atoms labeled.
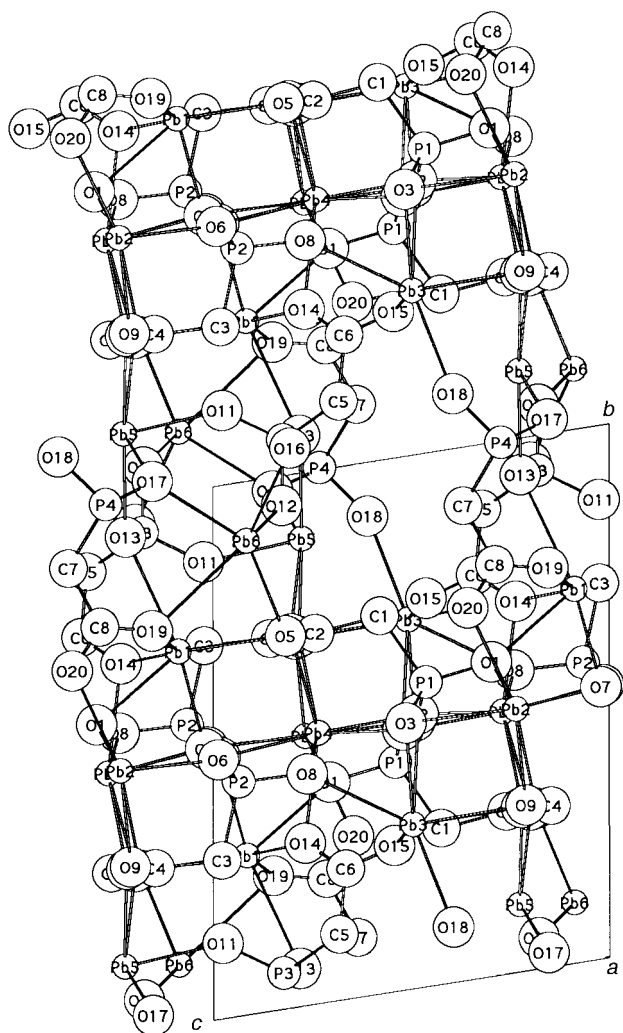
Fig. 7 Crystal structure of Pb$_6$(O$_3$PCH$_2$CO$_2$)$_4$ down to the *a*-axis with the numbering scheme used in Table 3. Only Pb–O bonds shorter than 2.95 Å are shown for clarity.

all in general positions. There are three crystallographically independent manganese atoms. Shannon average Mn^{II}-O bond distances are 2.15 Å for four-fold oxygen coordinations, and 2.23 Å for six-fold oxygen coordinations. If it is assumed that Mn–O interactions take place within 15% of the reported average Mn^{II}–O bond distances, then, three types of manganese coexist in this structure. Although somewhat arbitrary, this assumption allows us to define the coordination polyhedra. Hence, Mn(1) is surrounded by five oxygens with bond distances ranging between 2.09 and 2.19 Å, with a long interaction to a sixth oxygen at 2.68 Å. Mn(2) is surrounded by four oxygens with bond distances between 2.12 and 2.17 Å, with two long interactions at 2.47 and 2.75 Å. Mn(3) is six-coordinate with bond distances between 2.06 and 2.40 Å. The two phosphonate groups are tetrahedral and the two carboxy groups are trigonal.

The crystal structure of Mn$_3$(O$_3$PCH$_2$CO$_2$)$_2$ viewed down the *c*-axis is displayed in Fig. 5. Infinite chains of oxide manganese polyhedra [Mn(1) and Mn(3)] run parallel to the *b*-axis, and share edges. The chains can be described as Mn(1)$_2$O$_8$ dimers linked to Mn(3)$_2$O$_8$ dimers by a common edge formed by O(1) and O(5). The Mn(1)─O(1)─Mn(3) and Mn(1)─O(5)─Mn(3) angles are 106.5 and 100.7°, respectively. Mn(1)$_2$O$_8$ dimers form by sharing of an edge with two symmetry equivalent Mn(1)─O(6)─Mn(1) angles of 103.2(4)°. Dimers Mn(3)$_2$O$_{10}$ also form by sharing an edge with two symmetry equivalent Mn(3)─O(2)─Mn(3) angles of 96.4(4)°. These edge-sharing infinite chains can

be schematically summarised as ⋯Mn(3)O(1)O(5)-Mn(1)O(6)O(6)Mn(1)O(1)O(5)Mn(3)O(2)O(2)Mn(3)⋯. It is of interest that all these oxygen atoms belong to the phosphonate groups. These chains are interconnected along the *a*-axis through the carboxy groups and the Mn(2)O$_4$ groups. Fig. 6 shows the crystal structure down to the *b*-axis from which the links of the chains along the *c*-axis through the oxygens of the phosphonates defining a layer can be seen (in the *bc* plane). The structure can be depicted as inorganic layers in the *bc*-plane formed by the manganese polyhedra sandwiched by acetophosphonate groups in an ordered way such that phosphonate heads always point to the more coordinated manganese groups and the carboxylate tails always point to the four-coordinate manganese atoms. In this sense, it can be conceived as a PLS but with no space between the inorganic layers. There are small cavities where the hydrogens of the CH$_2$ groups [C(1) and C(3)] are located (Fig. 6); there is not enough empty space even for water molecules.

The crystal structure of Pb$_6$(O$_3$PCH$_2$CO$_2$)$_4$ contains 38 atoms in the asymmetric of the unit cell, all in general positions and there are six crystallographically independent lead atoms. To define the oxygen polyhedra around these lead atoms is more difficult than in the Mn case owing to the irregular geometry around Pb^{2+}. It is also important to keep in mind the possible lone-pair effect of Pb^{II} which has very important implications in coordination environment. It has been assumed that Pb–O interactions occur for distances >15% of the Shannon average Pb^{II}–O bond distance in an eight-fold oxygen coordination resulting in a limiting Pb–O bond distance of 3.09 Å. Shannon average Pb–O bond distances in 5, 6, 7, 8, 9 and 10 oxygen coordinations are: 2.59, 2.61, 2.63, 2.69, 2.75 and 2.80 Å, respectively. The Pb–O bond distances are given in Table 4. With this criterion, there are two five-, two eight- and two nine-coordinated lead atoms. It is of note that both five-coordinated lead atoms have two oxygens at quite short interacting distances of *ca.* 3.15 Å so they may be conceived as six- or even seven-coordinated (see Table 4). As for the manganese compound, the four phosphonate groups are tetrahedral and the four carboxy groups are trigonal.

The structure of Pb$_6$(O$_3$PCH$_2$CO$_2$)$_4$ (Fig. 7) is fairly similar to that of the manganese analogue. This is expected as both compounds have the same stoichiometry and the same organo-inorganic covalent building block [O$_3$PCH$_2$CO$_2$]$^{3-}$. For M = Pb, there are also two types of lead layers with higher and lower oxygen coordination numbers. One layer is formed by Pb(1)─Pb(4) which are eight and nine-coordinated. The other type of layer is built up of Pb(5) and Pb(6) which are five-coordinate. However, the arrangements of the carboxy phosphonate chains between these layers are different in both materials. To satisfy the coordination requirement around the lead layer with lower coordination number, two carboxy phosphonate chains point with the phosphonate heads towards this layer and the tails to the other type of lead layer.

To summarise, we have studied two acetophosphonates, Mn$_3$(O$_3$PCH$_2$CO$_2$)$_2$ and Pb$_6$(O$_3$PCH$_2$CO$_2$)$_4$, which show high thermal stability. Although the syntheses were carried out at low pH (4.3 and 1.8, respectively) they do not result in free carboxylic groups which would presumably result in more open structure. These structures are different and clearly more compact than those shown by their analogous 2-carboxyethylphosphonates, *i.e.* Zn$_3$[O$_3$P(CH$_2$)$_2$CO$_2$]$_2$[18b] and Co$_3$(O$_3$PC$_2$H$_4$CO$_2$)$_2$·6H$_2$O.[21] This is mainly due to the presence of an extra methylene group which leads to a more hydrophobic region which pillars the metal layers.

References

1 A. Clearfield, *Prog. Inorg. Chem.*, 1998, **47**, 371; S. Drumel, V. Penicaud, D. Deniaud and B. Bujoli, *Trends Inorg. Chem.*, 1996, **4**, 13.

2 J. M. Troup and A. Clearfield, *Inorg. Chem.*, 1977, **16**, 3311.

3 (*a*) D. Grohol and A. Clearfield, *J. Am. Chem. Soc.*, 1997, **119**, 4662; (*b*) D. Grohol, M. A. Subramanian, M. D. Poojary and A. Clearfield, *Inorg. Chem.*, 1996, **35**, 5264.

4 B. Bujoli, P. Palvadeau and J. Rouxel, *Chem. Mater.*, 1990, **2**, 582.

5 (*a*) L. J. Bideau, C. Payen, P. Palvadeau and B. Bujoli, *Inorg. Chem.*, 1994, **33**, 4885; (*b*) S. Drumel, P. Janvier, D. Deniaud and B. Bujoli, *J. Chem. Soc., Chem. Commun.*, 1995, 1051.

6 (*a*) K. Maeda, J. Akimoto, Y. Kiyozumi and F. Mizukami, *Angew. Chem. Int. Ed. Engl.*, 1995, **34**, 1199; (*b*) K. Maeda, J. Akimoto, Y. Kiyozumi and F. Mizukami, *J. Chem. Soc., Chem. Commun*, 1995, 1033.

7 (*a*) M. D. Poojary, A. Cabeza, M. A. G. Aranda, S. Bruque and A. Clearfield, *Inorg. Chem.*, 1996, **35**, 1468; (*b*) M. D. Poojary, D. Grohol and A. Clearfield, *Angew. Chem., Int. Ed. Engl.*, 1995, **34**, 1508.

8 M. D. Poojary, H. L. Hu, F. L. Campbell III and A. Clearfield, *Acta Crystallogr., Sect. B*, 1993, **49**, 996.

9 (*a*) G. Cao, H. Lee, V. M. Lynch, T. E. Mallouk, *Inorg. Chem.*, 1988, **27**, 2781; (*b*) G. Cao, H. Lee, V. M. Lynch, J. S. Swinnea and T. E. Mallouk, *Inorg. Chem.*, 1990, **29**, 2112; (*c*) A. Cabeza, M. A. G. Aranda, M. Martinez-Lara, S. Bruque and J. Sanz, *Acta Crystallogr., Sect. B*, 1996, **52**, 982.

10 (*a*) D. M. Poojary, B. Zhang, P. Bellinghausen and A. Clearfield, *Inorg. Chem.*, 1996, **35**, 4942; (*b*) A. Cabeza, M. A. G. Aranda, S. Bruque, M. D. Poojary, A. Clearfield and J. Sanz, *Inorg. Chem.*, 1998, **37**, 4168.

11 R. W. Murray, *Acc. Chem. Res.*, 1980, **13**, 135.

12 J. S. Facci, *Langmuir*, 1987, **3**, 525.

13 G. G. Roberts, *Adv. Phys.*, 1985, **34**, 475.

14 (*a*) M. Gratzel, *Pure Appl. Chem.*, 1982, **54**, 2369; (*b*) J. K. Thomas, *Acc. Chem. Res.*, 1988, **21**, 275.

15 M. A. Richard, J. Deustsch and G. M. Whitesides, *J. Am. Chem. Soc.*, 1979, **100**, 6613.

16 H. Byrd, A. Clearfield, D. Poojary, K. P. Reis and M. E. Thompson, *Chem. Mater.*, 1996, **8**, 2239.

17 (*a*) M. B. Dines, R. E. Cooksey, P. C. Griffith and R. H. Lane, *Inorg. Chem.*, 1983, **22**, 1003; (*b*) G. Alberti, R. Costantino, F. Marmottini and Z. P. Vivaniv, *Angew. Chem., Int. Ed. Engl.*, 1993, **32**, 1357; (*c*) G. Alberti, F. Marmottini, S. Murcia-Mascaros and R. Vivani, *Angew. Chem., Int. Ed. Engl.*, 1994, **33**, 1594; (*d*) M. E. Thompson, *Chem. Mater.*, 1994, **6**, 1168; (*e*) D. M. Poojary, B. Zhang, P. Bellinghausen and A. Clearfield, *Inorg. Chem.*, 1996, **35**, 5254.

18 (*a*) G. Cao, L. K. Rabenberg, C. M. Nunn and T. E. Mallouk, *Chem. Mater.*, 1991, **3**, 149; (*b*) S. Drumel, P. Janvier, P. Barboux, M. Bujoli-Doeuff and B. Bujoli, *Inorg. Chem.*, 1995, **34**, 148; (*c*) P. Janvier, S. Drumel, P. Piffard and B. Bujoli, *C. R. Acad. Sci. Paris, Ser. II*, 1995, **320**, 29.

19 T. Kijima, S. Watanabe and M. Machida, *Inorg. Chem.*, 1994, **33**, 2586.

20 (*a*) B. Bujoli, A. Courilleau, P. Palvadeau and J. Rouxel, *Eur. J. Solid State Inorg. Chem.*, 1992, **92**, 171; (*b*) S. Drumel, M. Bujoli-Doueff, P. Janvier and B. Bujoli, *New J. Chem.*, 1995, **19**, 239.

21 A. Dilster and S. C. Sevov, *Chem. Commun.*, 1998, 959.

22 A. Cabeza, M. A. G. Aranda, M. Martínez-Lara and S. Bruque, *Mater. Sci. Forum*, 1996, **228**, 165.

23 M. A. G. Aranda, E. R. Losilla, A. Cabeza and S. Bruque, *J. Appl. Crystallogr.*, 1998, **31**, 16.

24 L. J. Bellamy, in *The Infra-red Spectra of Complex Molecules*, Chapman and Hall, London, 1975.

25 P. E. Werner, L. Eriksson and M. Westdahl, *J. Appl. Crystallogr.*, 1985, **18**, 367.

26 P. M. Wolff, *J. Appl. Crystallogr.*, 1968, **1**, 108.

27 G. S. Smith and R. L. Snyder, *J. Appl. Crystallogr.*, 1979, **12**, 60.

28 A. C. Larson and R. B. von Dreele, Program version: PC, summer 96, Los Alamos National Lab. Rep. No. LA-UR-86-748, 1994.

29 A. Le Bail, H. Duroy and J. L. Fourquet, *Mater. Res. Bull.*, 1988, **23**, 447.

30 P. Thompson, D. E. Cox and J. B. Hasting, *J. Appl. Crystallogr.*, 1987, **20**, 79.

31 L. W. Finger, D. E. Cox and A. P. Jephcoat, *J. Appl. Crystallogr.*, 1994, **27**, 892.

32 A. Altomare, G. Cascarano, C. Giacovazzo, A. Guagliardi, M. Burla, G. Polidori and M. Camalli, SIRPOW92, *J. Appl. Crystallogr.*, 1994, **27**, 435.

33 G. M. Sheldrick, SHELXS86. Program for the Solution of Crystal Structures, University of Göttingen, Germany, 1985.

34 W. Dollase, *J. Appl. Crystallogr.*, 1986, **19**, 267.

35 H. M. Rietveld, *J. Appl. Crystallogr.*, 1969, **2**, 65.

Paper 8/04626C